

RAY-UI: New Features and Extensions

P. Baumgärtel^{1, a)}, P. Grundmann², T. Zeschke¹, A. Erko¹, J. Viefhaus¹, F. Schäfers¹
and H. Schirmacher²

¹*Department Optics and Beamlines
Helmholtz Zentrum Berlin für Materialien und Energie
Albert-Einstein-Str. 15, D-12489 Berlin,*
²*Fachbereich VI – Informatik und Medien
Beuth Hochschule für Technik Berlin,
Luxemburger Str. 10, D-13353 Berlin*

^{a)} Corresponding author: peter.baumgaertel@helmholtz-berlin.de

Abstract. The RAY-UI project started as a proof-of-concept for an interactive and graphical user interface (UI) for the well-known ray tracing software RAY [1]. In the meantime, it has developed into a powerful enhanced version of RAY that also serves as platform for new development, code optimization, and improvement of associated tools [2].

Compared to RAY several extensions and features were implemented: We introduced mono-capillaries and hyperbolic mirrors as new optical elements, and added a “Simple Undulator” as a new light source. Furthermore, we have extended the modelling of Reflection Zone Plates, and added support for SPECTRA [3] files for “Undulator File” light sources. Besides this RAY-UI is now also supporting “smart” parameters which apply to the whole optical system. As an example we show the setup of a plane-grating monochromator beamline in SX-700 mount, where the position of the premirror is calculated automatically according to the c-factor and the grating parameters. As an outlook, we show first results of automatically generated schematic beamline views.

EXTENDED SMART PARAMETERS

With RAY-UI we have introduced smart parameters which allow an efficient interaction, as they are functionally interconnected [2]. By default these interconnections occur only within the same optical element. Special optical systems sometimes require more complex functional dependencies. Thus we have extended the behavior of smart parameters in a way that optical elements of a beamline can “know” each other and can have functional, “smart” interconnections among themselves.

"Beamline Mount" - full simulation of a Plane Grating Monochromator

So far we have introduced this new property in the parameter “Beamline Mount”, which is available in the optical element “Plane Mirror” and “Plane Grating”. Switching this parameter in both elements from “standalone” to “SX700” allows simulating a plane-grating monochromator in SX700-mount based on the formulae of Pimpale [4]. In case one of the optical elements is not automatically detected (because the user has not finalized creating the beamline yet) a warning is displayed just beneath the parameter. Otherwise parameters are enabled for describing the SX700-mounts (see Fig. 1). We plan to implement a similar approach for normal incidence monochromators soon.

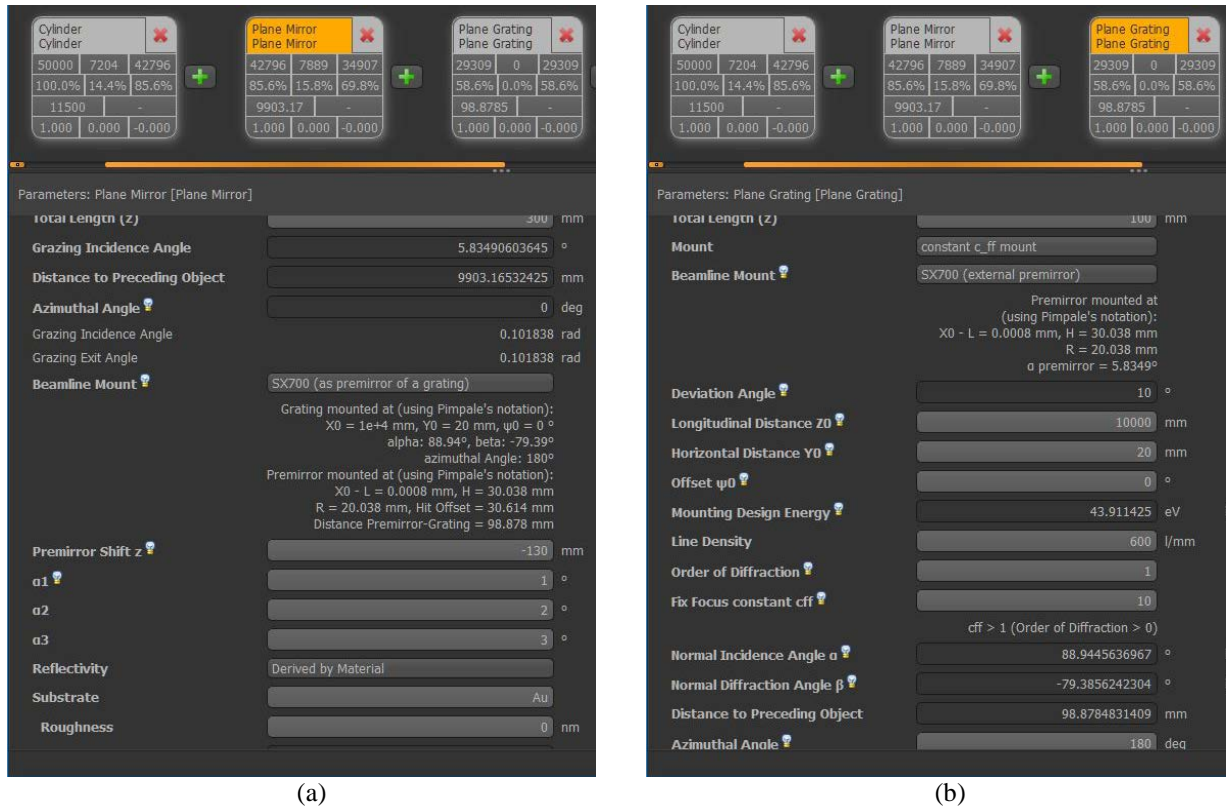


FIGURE 1. Parameter settings using the extended smart parameter “Beamline Mount” for simulating a plane grating monochromator in SX700-mount. The “Plane Mirror” is functionally connected with the “Plane Grating”. (a) “Parameter View” of the “Plane Mirror”, (b) of the “Plane Grating”.

ADDITIONAL OPTICAL ELEMENTS

Within the last years, we got several requests from the user community for new optical elements. Here we want to present the most important ones:

Hyperboloid

A two-sheeted hyperboloid can be described very much like an ellipsoid. As usual in RAY the surface is represented in its implicit form:

$$-\frac{z}{A^2} + \frac{y}{B^2} + \frac{x}{C^2} + 1 = 0 \quad (1)$$

From this we can derive the parameters of the general equation for a second-order surface, see [1]:

TABLE 1. Parameters of the general second-order surface equation in RAY’s coordinate system of the mirror [1]:	
Parameter	Hyperboloid
a11	$\frac{B^2}{C^2}$
a22	1

a_{33}	$-\frac{B^2}{A^2}$
$a_{12}, a_{13}, a_{23}, a_{14}$	0
a_{24}	y_0
a_{34}	$-\frac{B^2 z_0}{A^2}$
a_{44}	$B^2 + y_0^2 - \frac{B^2 z_0^2}{A^2}$

The curvature of the hyperbolic mirror can either be defined directly via its axes A, B, and C, or by its optical design parameters as geometrical focusing lengths (entrance arm length and exit arm length, L_{en} and L_{ex}) and the grazing incidence angle θ . For the sake of completeness, we have to consider four cases:

1. Concave, right sheet: $L_{en} > 0; L_{ex} < 0; |L_{en}| < |L_{ex}|$
2. Concave, left sheet: $L_{en} < 0; L_{ex} > 0; |L_{en}| > |L_{ex}|$
3. Convex, left sheet: $L_{en} < 0; L_{ex} > 0; |L_{en}| < |L_{ex}|$
4. Convex, right sheet: $L_{en} > 0; L_{ex} < 0; |L_{en}| > |L_{ex}|$

As examples, Fig. 2 shows cases 1 and 4. Typically, only case 1 is used in optical systems in combination with an ellipsoid, see [5].

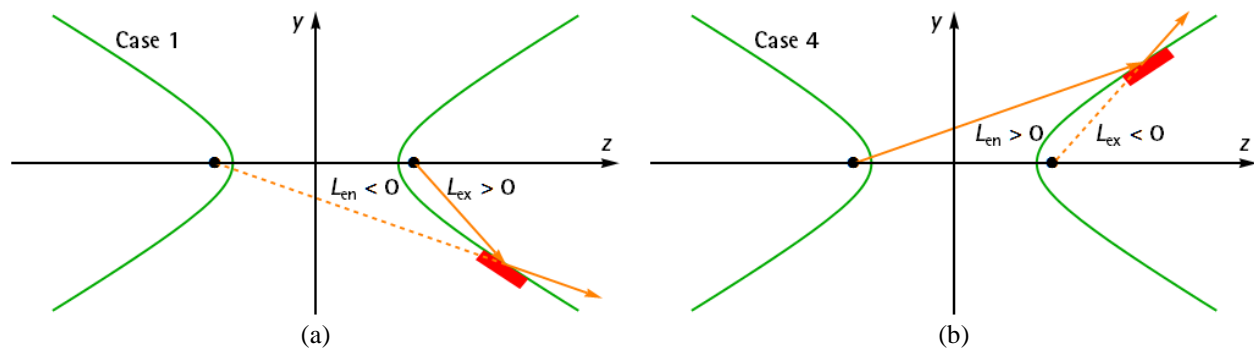


FIGURE 2. Schematic view of the imaging properties of an hyperbolic mirror in the coordinate system of the hyperbola. The green line shows the hyperbolic curvature, the black points the two foci, one of it is always a virtual focus, which is symbolized by its negative focus length shown as a yellow dashed line. The yellow solid line is the light beam. (a) illustrates case 1, (b) case 4.

Elliptical Monocapillary

We started to implement the new optical element “Monocapillary” for simplifying the parameter input for such a special kind of mirror compared to earlier versions of RAY. In this first release we have concentrated on elliptical monocapillaries, which are based on the formulae of an ellipsoidal mirror. The optical surface of the capillary can be fully defined by its length, inner diameter at entrance and its imaging properties, the focal entrance and exit arm length, L_{en} and L_{ex} , see Fig 3. Unlike the elliptical mirror the focal lengths are defined along the z-coordinate of the ellipsoid, and not along the incident and reflected beam toward the surface. As usual, rays that do not interact with the surface are discarded. This also applies to the rays that pass the capillary through the middle, thus there is no need to model the beam-stop that monocapillaries are usually equipped with.

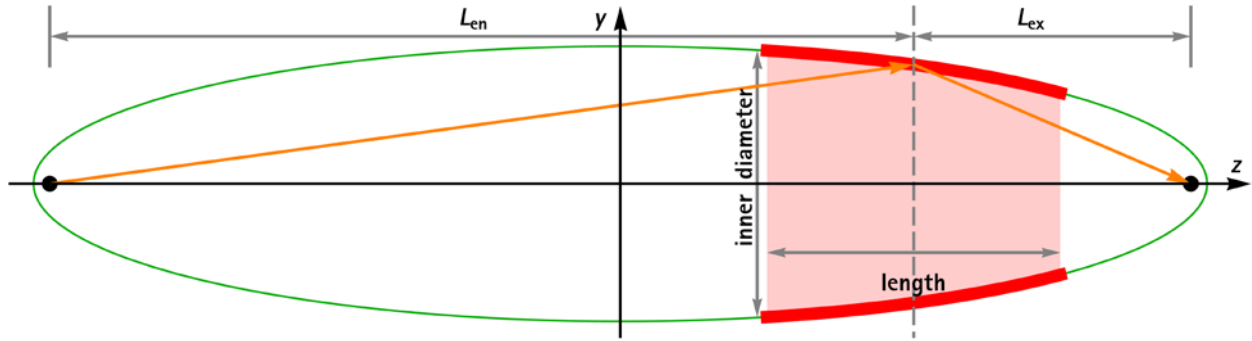


FIGURE 3. Schematic view of an elliptical monocapillary. The red area shows the capillary, the green line the elliptical curvature, the black points the two foci. The entrance length L_{en} and exit length L_{ex} are defined as distance of the source point (focus point on the left) to the middle of the capillary (dashed line) along the z -axes and as the distance of that point to the image point (focus on the right), respectively. The yellow solid line symbolizes one of the possible ray paths.

Simple Undulator

A further request of the users concerning light sources is to have an undulator source which works out of the box. Which means that no additional software is needed to derive the ray distribution, as it is the case for the source “Undulator File” (see Section Undulator File below). As a first step for this feature we introduced a new light source “Simple Undulator”, which is based on RAY-UI’s “Point Source”. The undulator source is approximated simply by a Gaussian distribution in space and divergence. The widths (Σ, Σ') of these distributions are described by the formulas of Elleaume [6] which only depend on the length of the undulator L , the wavelength λ and the convolution with the width of distribution of size σ_e and divergence σ'_e of the Gaussian-approximated electron beam.

$$\Sigma^2 = \sigma_e^2 + \frac{\lambda L}{2\pi^2} \quad (2)$$

$$\Sigma'^2 = \sigma'_e{}^2 + \frac{\lambda}{2L} \quad (3)$$

This approximation of an undulator source is restricted to on-axis radiation of the first harmonic only.

EXTENDED ELEMENTS

Undulator File

We have rewritten and extended the light source “Undulator File”: As input this undulator source requires an intensity distribution of an undulator from one single electron at a certain distance. This distribution must be calculated with special programs. We now support undulator files from WAVE [7], SPECTRA [3] and URGENT [8]. In all cases also relevant data of the header can be automatically transferred into RAY-UI. Photon source size and divergence are simulated by convolution of the one-electron emission spectrum with electron beam size and divergence.

Reflection Zone Plate (RZP)

The usefulness of RZPs in beamlines and spectrometers has been further advanced in recent years. Following these developments we also extended the “Reflection Zone Plate” in RAY-UI. Here we just want to list the new advanced features in keywords:

- illumination offset correction
- line density either derived by analytical formulae or provided by coefficients of a two dimensional polynomial
- analytical formulae for the design type "Fresnel Center Offset" or "Design Angle beta"

- 16 different imaging types available
- beside planar RZP also spherical and toroidal curvatures are supported

OUTLOOK

In this outlook, we only want to call attention to future extensions that are currently under development and will be available soon.

Schematic Beamline View

The visualization of an optical system is essential in the phase of designing. For example, errors in geometrical design can be detected more easily. But the visualization of a whole beam line in real world coordinates has its pitfalls because the size along the beam (z) is several orders of magnitude larger than perpendicular to the beam (x or y). Thus usually one can either visualize the entire beamline without recognizing any details, or zoom in on a single optical element while losing the overview. To overcome this disadvantage, we plan to integrate two beamline visualization modes directly into RAY-UI: linear mode for proportional visualization, and scaled mode for a schematic view (see Fig. 4). The new views will be available in live-update mode. A further goal is the integration of traced rays in order to support tasks like analyzing focus positions.

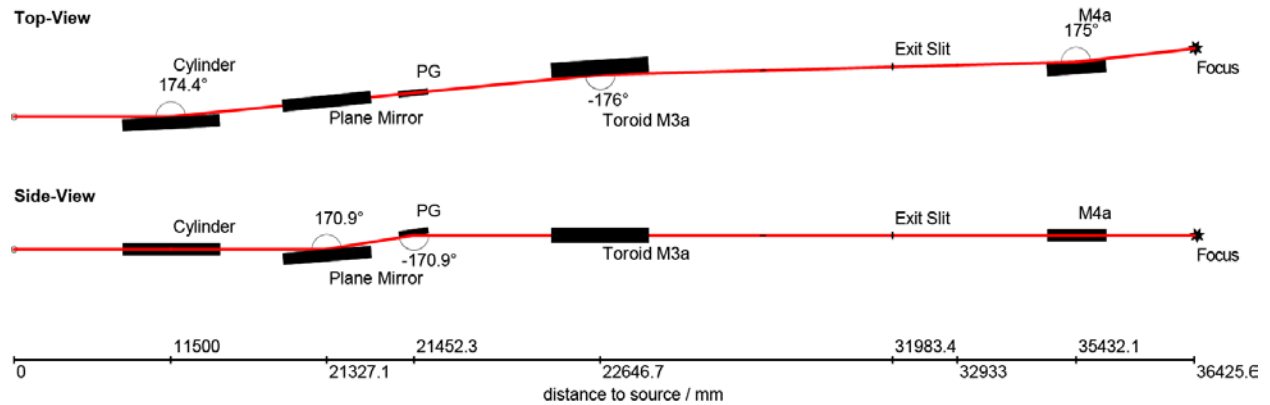


FIGURE 4: Preview of the “Beamline View” tool. Please note that this feature is still under development.

REFERENCES

1. F. Schäfers, “RAY - The BESSY Raytrace Program”, in: Modern Developments in X-Ray and Neutron Optics, Springer Series in Modern Optical Sciences, eds A. Erko, M. Idir, Th. Krist, A.G. Michette, Vol. 137, 9-41 (2008)
2. P. Baumgärtel, M. Witt, J. Baensch, M. Fabarius, A. Erko, F. Schäfers and H. Schirmacher, SRI 2016, AIP Conf. Proc. 1741, 040016 (2016)
3. <http://spectrax.org/spectra/> (2018/06/07)
4. Pimpale et al. Applied Optics 30, No. 13, 1591 (1991)
5. T. Warwick et al., Journal of Synchrotron Radiation 21, 736-743 (2014)
6. P. Elleaume, “Undulator radiation”, in: Undulators, Wigglers and their Applications, eds H. Onuki and P. Elleaume, Taylor & Francis, London, (2003)
7. https://www.helmholtz-berlin.de/forschung/oe/fg/undulatoren/arbeitsgebiete/wave_en.html (2018/06/07)
8. R. W. Walker and B. Diviacco, Review of Scientific Instruments 63, 392 (1992)